Chapter 5
# Cable and Compartmental Models of Dendritic Trees

IDAN SEGEV

5.1   Introduction

In the previous chapter, we used a single compartment model to study the mechanisms for the activation of voltage-activated channels, which produce neuron firing. Next, we need to understand how inputs to the neuron affect the potential in the soma and other regions that contain these channels. The following chapter deals with the response of the neuron to synaptic inputs to produce postsynaptic potentials (PSPs). In this chapter, we concentrate on modeling the spread of the PSP through the dendritic tree.

Dendrites are strikingly exquisite and unique structures. They are the largest component in both surface area and volume of the brain and their specific morphology is used to classify neurons into classes: pyramidal, Purkinje, amacrine, stellate, etc. (Fig. 5.1). But most meaningful is that the majority of the synaptic information is conveyed onto the dendritic tree and it is there where this information is processed. Indeed, dendrites are the elementary computing device of the brain.

A typical dendritic tree receives approximately ten thousand synaptic inputs distributed over the dendritic surface. When activated, each of these inputs produces a local conductance change for specific ions at the postsynaptic membrane, followed by a flow of the corresponding ion current between the two sides of the postsynaptic membrane. As a result, a local change in membrane potential is generated and then spreads along the dendritic branches. How does this spread depend on the morphology (the branching pattern) of the
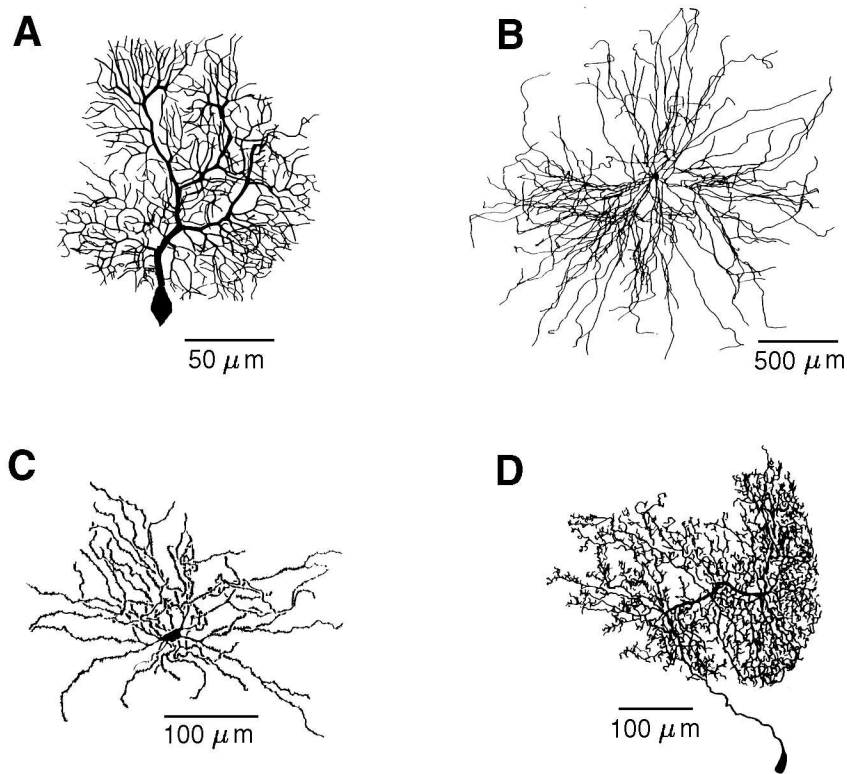
Figure 5.1   Dendrites have unique shapes which are used to characterize neurons into types. (A) Cerebellar Purkinje cell of the guinea pig (reconstructed by Moshe Rapp), (B) α-motoneuron from the cat spinal cord (reconstructed by Robert Burke), (C) Neostriatal spiny neuron from the rat (Wilson 1992), (D) Axonless interneurons of the locust (reconstructed by Giles Laurent). In many neuron types, synaptic inputs from a given source are preferentially mapped into a particular region of the dendritic tree. For example, in Purkinje cells, one excitatory input comes from the vast number of synapses (more than 100,000) that specifically contact spines on the thin tertiary branches, whereas the other excitatory input comes from the climbing fiber that contacts the thick (smooth) dendrites. Inhibition from the basket cells impinges close to the Purkinje cell soma, whereas inhibition from stellate cells contacts mainly distal parts of the tree. Note the differences in scales for the different neuron types.

tree and on the electrical properties of its membrane and cytoplasm? This question is a fundamental one; its answer will provide the understanding of how the various synaptic inputs that are distributed over the dendritic tree interact in time and in space to determine the input-output properties of the neuron and, consequently, their effect upon the computational capability of the neuronal networks that they constitute.

Cable theory for dendrites was developed in 1959 by W. Rall precisely for this purpose. Namely, to derive a mathematical model that describes the flow of electric current (and the spread of the resultant voltage) in morphologically and physiologically realistic dendritic trees that receive synaptic inputs at various sites and times. In the last thirty years, cable theory for dendrites, complemented by the compartmental modeling approach (Rall 1964), played an essential role in the estimation of dendritic parameters, in designing and interpreting experiments and in providing insights into the computational function of dendrites. This chapter attempts to briefly summarize cable theory and compartmental models, and to highlight the main results and insights obtained from applying cable and compartmental models to various neuron types. A complete account of Rall's studies, including his principal papers, can be found in Segev, Rinzel and Shepherd (1995).

We begin by getting acquainted with dendrites, the subject matter of this chapter. We then introduce the concepts and assumptions that led to the development of cable theory and then introduce the cable equation. Next, we discuss the implication of this equation for several important theoretical cases as well as for the fully reconstructed dendritic tree. The numerical solution of the cable equation using compartmental techniques is then presented. We summarize the chapter with the main insights that were gained from implementing cable and compartmental models with neurons of various types. Along the way, and at the end of the chapter, we suggest several exercises using GENESIS that will help the reader to understand the principles that govern signal processing in dendritic trees.

5.2 Background

5.2.1 Dendritic Trees: Anatomy, Physiology and Synaptology

Following the light microscopic studies of the phenomenal neuro-anatomist, Ramón y Cajal, dendrites became the focus of many anatomical investigations and today, with the aid of electron micrograph studies and computer-driven reconstructing techniques, we have a rather intimate knowledge of the fine structure of dendrites. These studies allowed us to obtain essential information on the exact site and type (excitatory or inhibitory) of synaptic inputs as well as on the dimensions of dendrites including the fine structures, the dendritic spines, that are involved in the synaptic processing (White 1989, Shepherd 1990). Here we attempt to introduce, in a concise way, some facts about dendrites and their synaptic inputs. One should remember that, because dendrites come in many shapes and sizes, such a summary unavoidably gives only a rough range of values; more information can be found

in Segev (1995).

Branching

Dendrites tend to bifurcate repeatedly and create (often several) large and complicated trees. Cerebellar Purkinje cells, for example, typically bear only one very complicated tree with approximately 400 terminal tips (Fig. 5.1A), whereas α-motoneurons from the cat spinal cord typically possesses 8–12 trees; each has approximately 30 terminal tips (Fig. 5.1B). The dendrites of each type of neurons have a unique branching pattern that can be easily identified and thus help to classify neurons.

Diameters

Dendrites are thin tubes of nerve membrane. Near the soma they start with a diameter of a few μm; their diameter typically falls below 1 μm as they successively branch. Many types of dendrites (e.g., cerebellar Purkinje cells, cortical and hippocampal pyramidals) are studded with abundant tiny appendages, the dendritic spines, which create very thin ($\sim 0.1 \mu m$) and short ($\sim 1 \mu m$) dendritic branches. When present, dendritic spines are the major postsynaptic target for excitatory synaptic inputs and they seem to be important loci for plastic processes in the nervous system (Rall 1974 in Segev et al. 1995, Segev and Rall 1988, Koch and Zador 1993).

Length

Dendritic trees may range from very short (100–200 μm, as in the spiny stellate cell in the mammalian cortex) to quite long (1–2 mm, for the spinal α-motoneurons). The total dendritic length may reach $10^4 \mu m$ (1 cm) and more.

Area and Volume

As mentioned in the introduction, the majority of the brain volume and area is occupied by dendrites. The surface area of a single dendritic tree is in the range of 2,000–750,000 μm^2; its volume may reach up to 30,000 μm^3.

Physiology of Dendrites

Both the intracellular cytoplasmic core and the extracellular fluid of dendrites are composed of ionic media that can conduct electric current. The membrane of dendrites can also conduct current via specific transmembrane ion channels, but the resistance to current flow across the membrane is much greater than the resistance along the core. In addition to the membrane channels (membrane resistance), the dendritic membrane can store ionic

charges, thus behaving like a capacitor. These R-C properties of the membrane imply a time constant ($\tau_m = RC$) for charging and discharging the transmembrane voltage. The typical range of values for τ_m is 1–100 *msec*. Also, the membrane and cytoplasm resistivity imply an input resistance (R_{in}) at any given point in the dendritic tree. R_{in} can range from 1 $M\Omega$ (at thick and leaky dendrites) and can reach 1000 $M\Omega$ (at thin processes, such as dendritic spines). The large values of R_{in} expected in dendrites imply that small excitatory synaptic conductance change (of ~ 1 nS) will produce, locally, a significant (a few tens of mV) voltage change. More details of the biophysics of dendrites, the specific properties of their membrane and cytoplasm and their electrical (rather than anatomical) length are considered below.

In classical cable theory, the assumption was that the electrical properties of the membrane and cytoplasmic properties are *passive* (voltage-independent) so that one could correctly speak of a membrane time *constant* and of a fixed input resistance (at a given site of the dendritic tree). However, recent recordings from dendrites (e.g., Stuart and Sakmann 1994) clearly demonstrate that the dendritic membrane of many neurons is endowed with voltage-gated ion channels. This complicates the situation (and makes it more interesting) since, now, the membrane resistivity (and thus τ_m and R_{in}) are voltage-dependent. For sufficiently large voltage perturbations, this nonlinearity may have important consequences on dendritic processing (Rall and Segev 1987). This important issue is further discussed below.

Synaptic Types and Distribution

Synapses are not randomly distributed over the dendritic surface. In general, inhibitory synapses are more proximal than excitatory synapses, although they are also present at distal dendritic regions and, when present, on some spines in conjunction with an excitatory input. In many systems (e.g., pyramidal hippocampal cells and cerebellar Purkinje cells), a given input source is preferentially mapped onto a given region of the dendritic tree (Shepherd 1990), rather being randomly distributed over the dendritic surface.

The time course of the synaptic conductance change associated with the various types of inputs in a given neuron may vary by 1–2 orders of magnitude. The fast excitatory (AMPA or non-NMDA) and inhibitory (GABA$_A$) inputs operate on a time scale of 1 *msec* and have a peak conductance on the order of 1 *nS*; this conductance is approximately 10 times larger than the slow excitatory (NMDA) and inhibitory (GABA$_B$) inputs that both act on a slower time scale of 10–100 *msec*.

5.2.2 Summary

Dendrites and their spines are the target for a large number of synaptic inputs that, in many cases, are non-randomly distributed over the dendritic surface. The dendritic membrane is equipped with a variety of synaptically activated and voltage-gated ion channels. The

kinetics and voltage dependence of these channels, together with a particular dendritic morphology and input distribution, make the dendritic tree behave as a complex *dynamical* device with a potentially rich repertoire of computational (input-output) capabilities. Cable theory for dendrites provides the mathematical framework that enables one to connect the morphological and electrical structure of the neuron to its function.

5.3 The One-Dimensional Cable Equation

5.3.1 Basic Concepts and Assumptions

As mentioned previously, dendrites are thin tubes wrapped with a membrane that is a relatively good electrical insulator compared to the resistance provided by the intracellular core or the extracellular fluid. Because of this difference in membrane vs. axial resistivity, for a short length of dendrite, the electrical current inside the core conductor tends to flow parallel to the cylinder axis (along the x-axis). This is why the classical cable theory considers only one spatial dimension (x) along the cable, while neglecting the y and z dimensions. In other words, one key assumption of the one-dimensional cable theory is that the voltage V across the membrane is a function of only time t and distance x along the core conductor.

The other fundamental assumptions in the classical cable theory are: (1) The membrane is passive (voltage-independent) and uniform. (2) The core conductor has constant cross section and the intracellular fluid can be represented as an ohmic resistance. (3) The extracellular resistivity is negligible (implying extracellular isopotentiality). (4) The inputs are currents (which sum linearly, in contrast to changes in synaptic membrane conductance, whose effects do not sum linearly, as we shall see in Chapter 6). For convenience, we will make the additional assumption that the membrane potential is measured with respect to a resting potential of zero, as we assumed in the previous chapter.

These assumptions allow us to write down the one-dimensional passive cable equation for $V(x,t)$, the voltage across the membrane cylinder at any point x and time t. As was shown by Rall (1959), this equation can be solved analytically for arbitrarily complicated passive dendritic trees. As noted before, real dendritic trees receive conductance inputs (not current inputs) and may possess nonlinear membrane channels (violating the passive assumption). Yet, as we discuss later, the passive case is very important as the essential reference case, and it provided the fundamental insights regarding signal processing in dendrites.

5.3.2 The Cable Equation

At any point along a cylindrical membrane segment (core conductor), current can flow either longitudinally (along the x-axis), or through the membrane. The longitudinal current I_i (in amperes) encounters the cytoplasm resistance, producing a voltage drop. We take this

current to be positive when flowing in the direction of increasing values of x, and define the *cytoplasm resistivity* as a resistance per unit length along the x-axis r_i, expressed in units of Ω/cm. Then, Ohm's law allows us to write

$$\frac{1}{r_i}\frac{\partial V}{\partial x} = -I_i. \tag{5.1}$$

The membrane current can either cross the membrane via the passive (resting) membrane channels, represented as a resistance r_m (in $\Omega \cdot cm$) for a unit length, or charge (discharge) the membrane capacitance per unit length c_m (in F/cm). If no additional current is applied from an electrode, then the change per unit length ($\partial I_i/\partial x$) of the longitudinal current must be the density of the membrane current i_m per unit length (taken positive outward),

$$\frac{\partial I_i}{\partial x} = -i_m = -(\frac{V}{r_m} + c_m\frac{\partial V}{\partial t}). \tag{5.2}$$

Combining Eq. 5.1 and Eq. 5.2, we get the cable equation, a second-order partial differential equation (PDE) for $V(x,t)$,

$$\frac{1}{r_i}\frac{\partial^2 V}{\partial x^2} = c_m\frac{\partial V}{\partial t} + \frac{V}{r_m}. \tag{5.3}$$

For the derivation of Eq. 5.3, it has been useful to consider the cytoplasm resistivity r_i, membrane resistivity r_m and membrane capacitance c_m for a unit length of cable having some fixed diameter. If we want to describe the cable properties in terms of the cable diameter, or we wish to make a compartmental model of a dendrite based on short sections of length l (Sec. 5.5), we will need expressions for the actual resistances and capacitance in terms of the cable dimensions.

It is often useful to refer to the membrane capacitance or resistance of a patch of membrane that has an area of 1 cm^2, so that our calculations can be independent of the size of a neural compartment. These quantities are called the *specific capacitance* and *specific resistance* of the membrane. In this book, and in the GENESIS tutorials, we denote the specific capacitance by C_M and the specific resistance by R_M, and use the symbols C_m and R_m for the actual values of the membrane capacitance and resistance of a section of dendritic cable in farads and ohms. This can be a point of confusion when reading other descriptions of cable theory, as it is also common to use the same notation (C_m and R_m) for the specific quantities.

The capacitance of biological membranes was found to have a specific value C_M close to 1 $\mu F/cm^2$. Hence, the actual capacitance C_m of a patch of cylindrical membrane with diameter d and length l is πdlC_M. In terms of the capacitance per unit length, $C_m = lc_m$. If the passive channels are uniformly distributed over a small patch of membrane, the conductance will be proportional to the membrane area. This means that the membrane resistance

will be inversely proportional to the area and that it can be written as $R_m = R_M/(\pi dl)$, or as $R_m = r_m/l$. R_M is then expressed in units of $\Omega \cdot cm^2$. Later in this chapter, we perform some simulations in which a number of cylindrical compartments are connected through their axial resistances R_a. As this resistance is proportional to the length of the compartment and inversely proportional to its cross sectional area, we can define a *specific axial resistance R_A* that is independent of the dimensions of the compartment and has units of $\Omega \cdot cm$. Thus, a cylindrical segment of length l and diameter d will have an axial resistance R_a of $(4lR_A)/\pi d^2$, or lr_i.

We can summarize these relationships with the equations

$$C_m = c_m l = \pi dl C_M, \tag{5.4}$$

$$R_m = r_m/l = \frac{R_M}{\pi dl} \tag{5.5}$$

and

$$R_a = r_i l = \frac{4lR_A}{\pi d^2}. \tag{5.6}$$

It is useful to define the *space constant*,

$$\lambda = \sqrt{r_m/r_i} = \sqrt{(d/4)R_M/R_A} \tag{5.7}$$

(in *cm*) and the *membrane time constant*,

$$\tau_m = r_m c_m = R_M C_M = R_m C_m. \tag{5.8}$$

Then, the cable equation (Eq. 5.3) becomes

$$\lambda^2 \frac{\partial^2 V}{\partial x^2} - \tau_m \frac{\partial V}{\partial t} - V = 0, \tag{5.9}$$

or in dimensionless units,

$$\frac{\partial^2 V}{\partial X^2} - \frac{\partial V}{\partial T} - V = 0, \tag{5.10}$$

where $X = x/\lambda$ and $T = t/\tau_m$. A complete derivation of the cable equation can be found in Rall (1989) and in Jack, Noble and Tsien (1975).

5.4   Solution of the Cable Equation for Several Cases

5.4.1   Steady-State Voltage Attenuation with Distance

The solution of Eq. 5.10 depends, in addition to the electrical properties of the membrane and cytoplasm, on the initial condition and the boundary condition at the end of the segment toward which the current flows. Consider the simple case of a steady state ($\partial V/\partial t = 0$); the cable equation (5.10) is reduced to an ordinary differential equation.

$$\frac{d^2V}{dX^2} - V = 0, \tag{5.11}$$

whose general solution can be expressed as

$$V(X) = Ae^X + Be^{-X}, \tag{5.12}$$

where A and B depend on the boundary conditions. In the case of a cylindrical segment of infinite extension, where $V = 0$ at $X = \infty$, and $V = V_0$ at $X = 0$, the solution for Eq. 5.11 is

$$V(X) = V_0 e^{-X} = V_0 e^{-x/\lambda}. \tag{5.13}$$

Thus, in this case, the steady voltage attenuates exponentially with distance. Indeed, in a very long uniform cylindrical segment, a steady voltage attenuates e-fold for each unit of λ. This holds only for a cylinder of infinite length.

Now, let us consider a finite length of dendritic cable. If it has a length l, we can define the dimensionless *electrotonic length* as $L = l/\lambda$. When the cylindrical segment has a sealed end at $X = L$ ("open circuit termination"), no longitudinal current flows at this end. Then, the solution for Eq. 5.11 with $V = V_0$ at $X = 0$ is

$$V(X) = \frac{V_0 \cosh(L-X)}{\cosh(L)}, \text{ for } \frac{\partial V}{\partial X} = 0 \text{ at } X = L. \tag{5.14}$$

As shown in Fig. 5.2, in finite cylinders with sealed ends, steady voltage attenuates less steeply than $\exp(-x/\lambda)$. In the other extreme, where the point $X = L$ is clamped to the resting potential (denoted here, for simplicity, as 0), the solution of Eq. 5.11 is

$$V(X) = \frac{V_0 \sinh(L-X)}{\sinh(L)}, \text{ for } V = 0 \text{ at } X = L. \tag{5.15}$$

In this case, steady voltage attenuates more steeply than the attenuation in the infinite case (Fig. 5.2). In dendritic trees, a dendritic segment typically ends with a subtree; this "leaky end" condition is somewhere between the sealed end (Eq. 5.14) and the "clamped to rest" condition (Eq. 5.15). (See Sec. 5.4.5.)
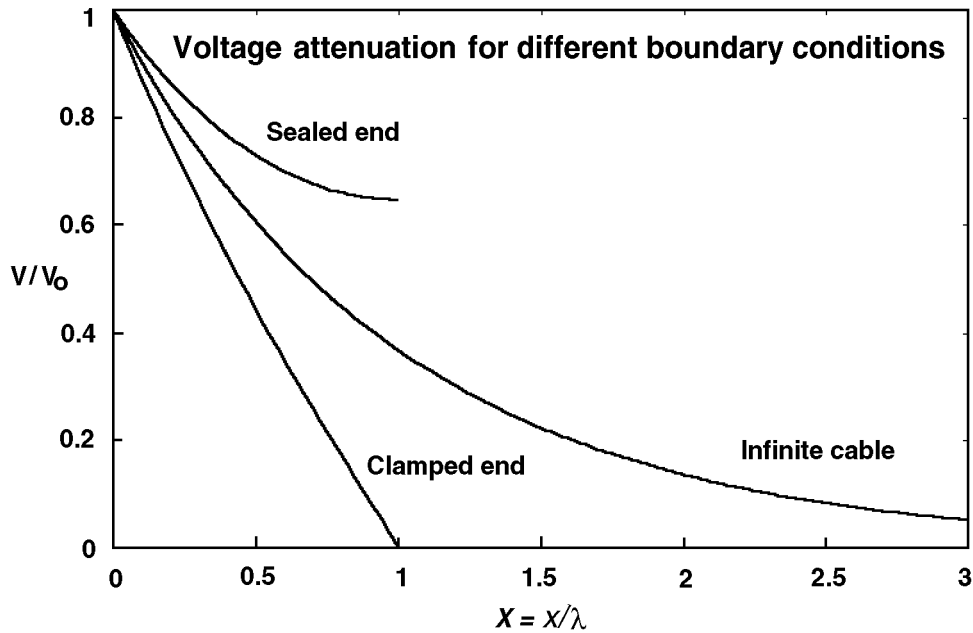
Figure 5.2   Attenuation of membrane potential with distance in a cylindrical cable with different boundary conditions. The middle curve shows the attenuation in an infinite cable (Eq. 5.13). The other two plots are for a finite length cable of electrotonic length $L = 1$. The upper one is for a sealed end cable (no current flows past the end, Eq. 5.14) and the lower is for a cable with the end clamped to the resting potential of 0 (Eq. 5.15).

5.4.2   Voltage Decay with Time

Consider the other extreme case of the cable equation (5.10) where $\partial V / \partial x = 0$. The cable is "shrunken" to an isopotential element, and Eq. 5.10 is reduced to an ordinary differential equation (ODE),

$$\frac{dV}{dT} + V = 0, \tag{5.16}$$

whose general solution can be expressed as

$$V(T) = Ae^{-T}, \tag{5.17}$$

where A depends on the initial condition. When a current step I_{pulse} is injected to this isopotential neuron, the resultant voltage V is

$$V(T) = I_{pulse}R_m(1 - e^{-T}) = I_{pulse}R_m(1 - e^{-t/\tau_m}), \tag{5.18}$$

where R_m is the net membrane resistance (in ohms) of this isopotential segment. At the cessation of the current at $t = t_0$, the voltage decays exponentially from its maximal value

$V_0 = V(t_0)$,

$$V(T) = V_0 e^{-T} = V_0 e^{-t/\tau_m}, \text{ for } t \geq t_0. \tag{5.19}$$

Equation 5.18 implies that, because of the R-C properties of the membrane, the voltage developed as a result of the current input lags behind the current input; Equation 5.19 implies that voltage remains for some time after the input ends ("memory"). This situation is discussed in more detail in Chapter 6.

In the general case of passive cylinders, the solution to the cable equation (Eq. 5.10) can be expressed as a sum of an infinite number of exponential decays,

$$V(X,T) = \sum_{i=0}^{\infty} B_i \cos(i\pi X/L) e^{-t/\tau_i}, \tag{5.20}$$

where the Fourier coefficients B_i depend only on L, the index i, and on the initial conditions (the input point and the initial distribution of voltage over the tree). The time constants τ_i are independent of location in the tree; $\tau_i < \tau_{i+1}$ for any i and, for the uniform membrane, the slowest time constant $\tau_0 = \tau_m$. The shorter ("equalizing") time constants (τ_i, for $i = 1$, $2, \ldots$) depend only on the electrotonic length L of the cylinder (in units of λ). Specifically, in cylinders of length L with a sealed end, they are given by

$$\tau_0/\tau_i = 1 + (i\pi/L)^2. \tag{5.21}$$

Consequently, Rall showed that L can be estimated directly from the values of τ_i, in particular from the two slowest time constants, τ_0 and τ_1, that can be "peeled" from the experimental voltage transient (Rall 1969). More details are given in reviews by Rall (1977, 1989) and Jack et al. (1975). You may observe this effect by doing Exercise 5 at the end of the chapter.

Rall also showed that the time course of synaptic potentials changes as the recording point moves away from the input location. The time course of the voltage response near the input site is relatively rapid and it becomes significantly prolonged (and attenuated) at a point distant from the input site. This effect is the source of Rall's method (Rall 1967) of using shape parameters of the synaptic potentials (its "rise time" and its width at half amplitude, the "half-width") to estimate the electrotonic distance of the synapse (the input) from the soma (the recording site). As shown in Fig. 5.3B and in Exercise 7, the more delayed the peak is, and the more "smeared" it is, the more distal the input (Rall 1967).

5.4.3   Functional Significance of λ and τ_m

The space constant λ and the membrane time constant τ_m are two very important parameters that play a critical role in determining the spatio-temporal integration of synaptic inputs in dendritic trees. Equation 5.19 shows that τ_m provides a measure of the time window for

input integration. A cell with large τ_m (e.g., 50 *msec*) integrates inputs over a larger time window compared to cells with smaller τ_m values (say, 5 *msec*). The value of τ_m depends on the electrical properties of the membrane R_M and C_M, but it does not depend on the cell morphology. Neurons with a high density of open membrane channels (i.e., with a small R_M value) will respond quickly to the input and will "forget" this input rapidly. In contrast, neurons with relatively few open membrane channels (large R_M) will be able to summate inputs for relatively long periods of time (slow voltage decay).

In contrast to τ_m, the space constant λ depends not only on the membrane properties but also on the specific axial resistance and the diameter. In neurons with large λ (e.g., with large R_M and/or large diameter, or small R_A) voltage attenuates less with distance as compared to neurons with a smaller λ value. Thus, in the former case, inputs that are anatomically distant from each other will summate better (spatially) with each other than in the latter case. Therefore, knowledge of λ and τ_m for a given neuron provides important information about the capability of its dendritic tree to integrate inputs both in time and in space.

5.4.4   The Input Resistance R_{in} and "Trees Equivalent to a Cylinder"

A third important parameter is R_{in}, the *input resistance* at a given point in the dendritic tree. When a steady current I_0 is applied at a given location in a structure, a steady voltage V_0 is developed at that point. The ratio V_0/I_0 is the input resistance at that point. This parameter is of great functional significance because it provides a measure for the "responsiveness" of a specific region to its inputs. It is also a quantity which, unlike R_M, may be directly measured. From Ohm's law, we know that a dendritic region with a large R_{in} requires only a small input current (a small excitatory conductance change) to produce a significant voltage change locally, at the input site. Conversely, a region with small R_{in} requires a more powerful input (or several inputs) to generate a significant voltage change locally.

In the case of an infinite cylinder, when a steady current input is injected at some point $x = 0$, the input current must divide into two equal core currents; one half flows to the right at $x = 0$ and the other half flows to the left. Thus, from Eq. 5.1,

$$I_i = -\frac{1}{r_i}\frac{\partial V}{\partial x}\bigg|_{x=0} = \frac{I_0}{2}. \tag{5.22}$$

From Eq. 5.13, the derivative $(\partial V/\partial x)|_{x=0} = -V_0/\lambda$. We then get,

$$R_{in} = V_0/I_0 = r_i\lambda/2 = \sqrt{r_m r_i}/2, \tag{5.23}$$

or

$$R_{in} = (1/\pi)d^{-3/2}\sqrt{R_M R_A}. \tag{5.24}$$

For the semi-infinite cylinder, the input resistance (often represented by R_∞) will be twice this amount. Hence, in an infinitely long cylinder, the input resistance is directly proportional to the square root of the specific membrane and axoplasm resistivities, and is inversely proportional to the core diameter, raised to the 3/2 power. Consequently, thin cylinders have a larger R_{in} compared to thicker cylinders that have the same R_M and R_A values. The dependence of the input resistance on $d^{3/2}$ was utilized by Rall (1959) to develop the concept of "trees equivalent to a cylinder". Rall argued that when a cylinder with diameter d_p bifurcates into two daughter branches with diameters d_1 and d_2 (and both daughter branches have the same boundary conditions at the same value of L), the branch point behaves as a continuous cable for current that flows from the parent to daughters, if

$$d_p^{3/2} = d_1^{3/2} + d_2^{3/2}. \qquad (5.25)$$

Provided that the specific properties of membrane and cytoplasm are uniform, Eq. 5.25 implies that the sum of input conductances of the two daughter branches (at the branch point) is equal to the input conductance of the parent branch at this point (impedance matching at the branch point). Thus, a branch point that obeys Eq. 5.25 is electrically equivalent to a uniform cylinder (looking from the parent into the daughters). Rall extended this concept to trees and showed that (from the soma viewpoint out to the dendrites) there is a subclass of trees that are electrically equivalent to a single cylinder whose diameter is that of the stem (near the soma) dendrite. (See Rall (1959, 1989) and Jack et al. (1975).) It was surprising to find that dendrites of many neuron types (e.g., the α-motoneuron in Fig. 5.1B) obey, to a first approximation, the $d^{3/2}$ rule (Eq. 5.25). (See, for example, Bloomfield, Hamos and Sherman (1987).) However, the dendrites of several major types of neurons (e.g., cortical and hippocampal pyramidal cells) do not obey this rule. Still, the "equivalent cylinder" model for dendritic trees allows for a simple analytical solution (Rall and Rinzel 1973, Rinzel and Rall 1974) and, indeed, it provided the main insights regarding the spread of electrical signals in passive dendritic trees, as summarized in Sec. 5.7.

It may be shown that the input resistance for a finite cylinder with sealed end at $X = L$ is larger by a factor of $\coth(L)$ than that of a semi-infinite cylinder having the same membrane and axial resistance, and the same diameter. When the end at $X = L$ is clamped to rest, the input resistance is smaller than that of the semi-infinite cylinder by a factor of $\tanh(L)$. (See Rall (1989) for complete derivations.) This leads to the useful result that, if the neuron and its associated dendritic tree can be approximated by an equivalent sealed end cylinder of surface area A and electrotonic length L, then

$$R_M = R_{in} A \tanh(L)/L. \qquad (5.26)$$

This provides a way to estimate the specific membrane resistance R_M from the measured input resistance if A and L are known, or to estimate the dendritic surface area if R_M and L are known (Rall 1977, 1989).

5.4.5 Summary of Main Results from the Cable Equation

In view of the solutions for the three representative cases, the infinite cylinder (Eq. 5.13), the finite cylinder with sealed end (Eq. 5.14) and the finite cylinder with end clamped to the resting potential (Eq. 5.15), it is important to emphasize a few points:

1. The attenuation of steady voltage is determined solely by the space constant λ, only in the case of infinite cylinders. In this case, steady voltage attenuates e-fold per unit of length λ. In finite cylinders, however, λ is not the sole determinant of this attenuation; the electrical length of the cylinder L and the boundary condition at the end toward which current flows (and voltage attenuates) also determine the degree of attenuation along the cylinder (Fig. 5.2).

2. The "sealed end" or "open circuit" boundary condition and the "clamped to rest" termination are two extremes. In dendritic trees, short dendritic segments terminate by a subtree that imposes "leaky" boundary conditions at the segment's ends. The size of the subtree and its electrical properties determine how leaky the conditions are at the boundaries of any given segment. In general, when a large tree is connected at the end of the dendritic segment, the leaky boundary condition at this end approaches the "clamped to rest" condition. When current flows in the direction of such a leaky end, voltage attenuates steeply along this segment. In contrast, when the subtree is very small the leaky boundary conditions approach the "sealed-end" condition and a very shallow attenuation is expected towards such an end (Fig. 5.3A). Rall (1959) showed how to compute analytically the various boundary conditions at any point in a passive tree with arbitrary branching and specified R_M, R_A and (for the transient case) C_M values (see also Jack et al. (1975), Segev et al. (1989)).

3. An important consequence of this dependence of voltage attenuation on the boundary conditions in dendritic trees is that this attenuation is asymmetric in the central (from dendrites to soma) vs. the peripheral (away from soma) directions. In general, because the boundary conditions are more "leaky" in the central direction, voltage attenuation in this direction is steeper than in the peripheral one. Figure 5.3A illustrates this important point very clearly.

4. Dendritic trees can be approximated (electrically), to a first degree, by a single (finite) cylinder. Therefore, analysis of the behavior of voltage in such cylinders provides important insights into the behavior of voltage in dendritic trees.

5. By peeling the slowest (τ_0) and the first equalizing time constant (τ_1) from somatic voltage transients, the electrical length L of the dendritic tree could be estimated, assuming that the tree is equivalent to a single cylinder (Eq. 5.21). Indeed, utilizing this peeling method for many neuron types we know that, depending on the neuron

type and experimental condition, *L* ranges between 0.3–2 (in units of λ). Thus, from the viewpoint of the soma, dendrites are electrically rather compact.
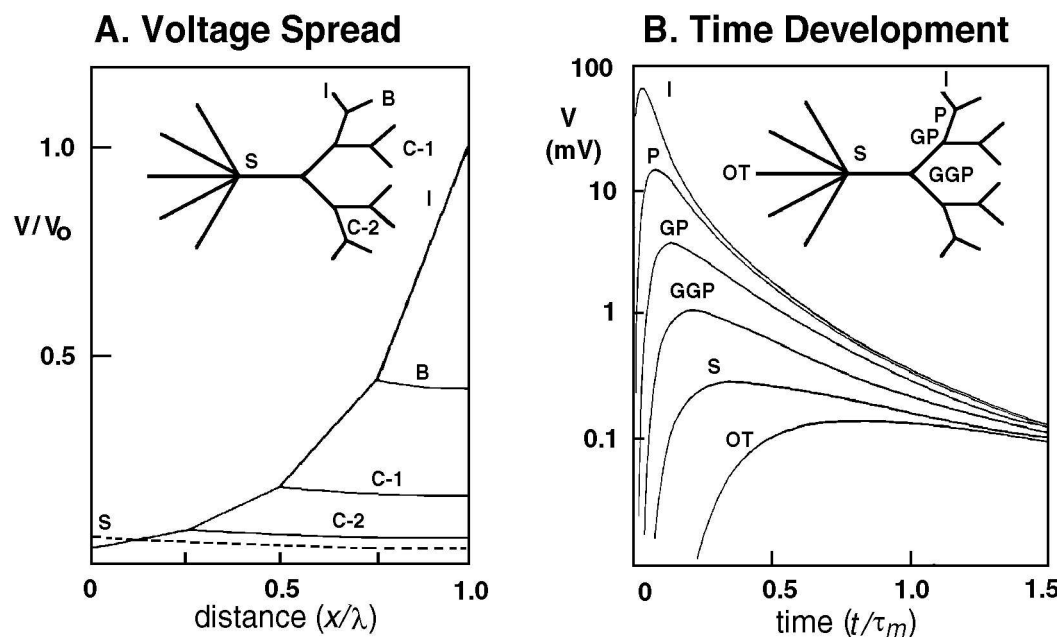
Figure 5.3 The voltage spread in passive dendritic trees is asymmetrical (A); its time-course changes (is broadened) and the peak is delayed as it propagates away from the input site (B). Solid curve in (A) shows the steady-state voltage computed for current input to terminal branch I. Large attenuation is expected in the input branch whereas much smaller attenuation exists in its identical sibling branch B. The dashed line corresponds to the same current when applied to the soma. Note the small difference, at the soma, between the solid curve and the dashed curve, indicating the negligible "cost" of placing this input at the distal branch rather than at the soma. (Data replotted from Rall and Rinzel (1973).) In (B), a brief transient current is applied to terminal branch I and the resultant voltage at the indicated points is shown on a logarithmic scale. Note the marked attenuation of the peak voltage (by several hundredfold) from the input site to the soma and the broadening of the transient as it spreads away from the input site. (Data replotted from Rinzel and Rall (1974).) Dendritic terminals have sealed ends in both (A) and (B).

5.5 Compartmental Modeling Approach

The compartmental modeling approach complements cable theory by overcoming the assumption that the membrane is passive and the input is current (Rall 1964). Mathematically, the compartmental approach is a finite-difference (discrete) approximation to the (nonlinear) cable equation. It replaces the continuous cable equation by a set, or a matrix, of ordinary differential equations and, typically, numerical methods are employed to solve this

system (which can include thousands of compartments and thus thousands of equations) for each time step. Conceptually, in the compartmental model dendritic segments that are electrically short are assumed to be isopotential and are lumped into a single R-C (either passive or active) membrane compartment (Fig. 5.4C). Compartments are connected to each other via a longitudinal resistivity according to the topology of the tree. Hence, differences in physical properties (e.g., diameter, membrane properties, etc.) and differences in potential occur between compartments rather than within them. It can be shown that when the dendritic tree is divided into sufficiently small segments (compartments) the solution of the compartmental model converges to that of the continuous cable model. A compartment can represent a patch of membrane with a variety of voltage-gated (excitable) and synaptic (time-varying) channels. A review of this very popular modeling approach can be found in Segev, Fleshman and Burke (1989).

As an example, consider a section of a uniform cylinder, divided into a number of identical compartments, each of length l. If we introduce an additional current I_j to represent the flow of ions from the jth compartment through active (nonlinear synaptic and/or voltage-gated) channels, we can write Eq. 5.3 as

$$\frac{l^2}{R_a}\frac{\partial^2 V_j}{\partial x^2} = C_m\frac{\partial V_j}{\partial t} + \frac{V_j}{R_m} + I_j. \tag{5.27}$$

Here, V_j represents the voltage in the jth compartment, and we have used Eqs. 5.4-5.6 to give the actual values of the resistances and capacitances (in ohms and farads) of this compartment, instead of the values for a unit length. Note that now R_m represents the membrane resistance at rest, before the membrane potential (and membrane resistance) is changed due to the current I_j. Also, note that V_j appears in the expression for I_j. For example, in the case of synaptic input to compartment j, $I_j = g(t)(V_j - E_{syn})$. Here, $g(t)$ and E_{syn} are synaptic conductance and reversal potential, respectively. (This is discussed in more detail in Sec. 6.3.1 of the following chapter.)

It can be shown by use of Taylor's series that for small values of l, the left hand side of Eq. 5.27 can be expressed in terms of differences between the value of V_j and the values in the adjacent compartments, V_{j-1} and V_{j+1}. In this approximation, the cable equation becomes

$$\frac{V_{j+1} - 2V_j + V_{j-1}}{R_a} = C_m\frac{dV_j}{dt} + \frac{V_j}{R_m} + I_j. \tag{5.28}$$

For the general case of a dendritic cable of non-uniform diameter (in which R_m, R_a and C_m may vary among compartments), we obtain the result given earlier in Eq. 2.1 and discussed in Sec. 2.2. This equation can easily be extended to include a branch structure. For a tree represented by N compartments we get N coupled equations of the form of Eq. 5.28. They should be solved simultaneously to obtain V_j, for $j = 1, 2, \ldots, N$ at each time step Δt.

A. Characterized Neuron

B. Cable Model

C. Compartmental Model
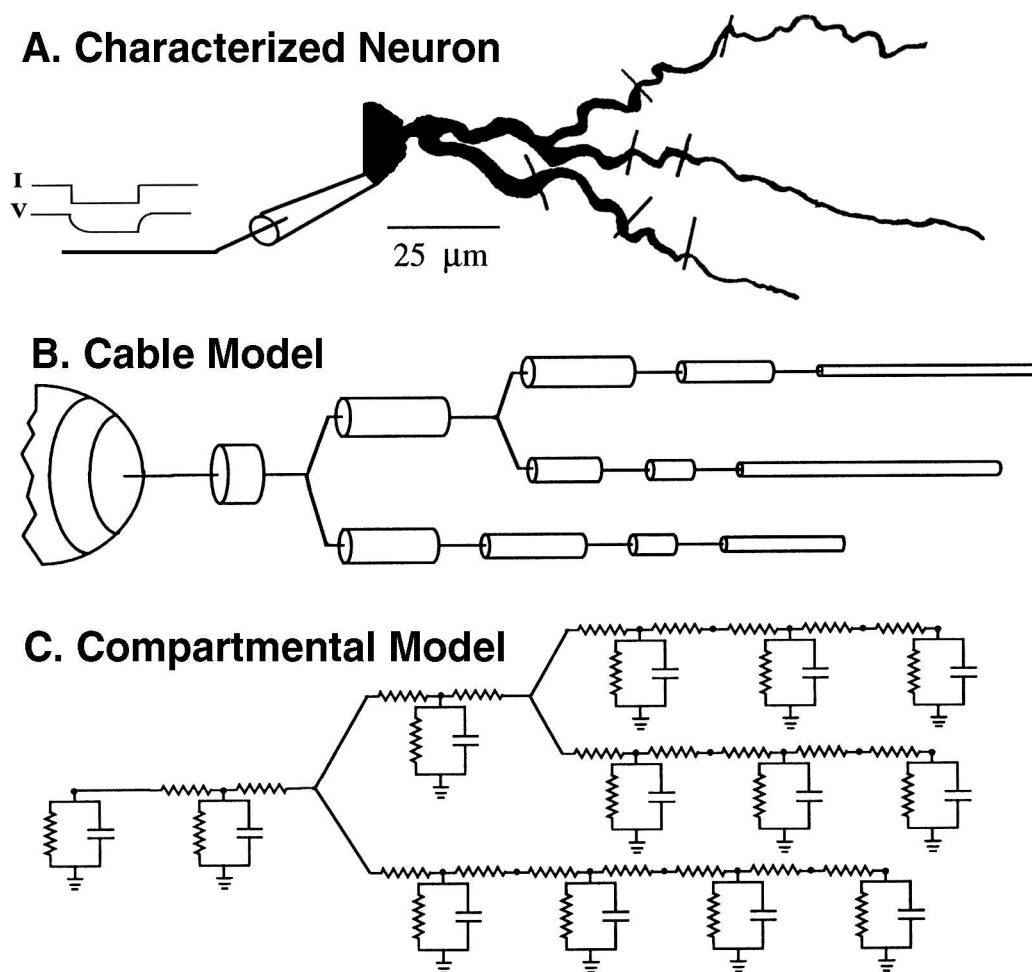
Figure 5.4   Dendrites (A) are modeled either as a set of cylindrical membrane cables (B) or as a set of discrete isopotential R-C compartments (C). In the cable representation (B), the voltage can be computed at any point in the tree by using the continuous cable equation and the appropriate boundary conditions imposed by the tree. An analytical solution can be obtained for any current input in passive trees of arbitrary complexity with known dimensions and known specifi c membrane resistance and capacitance (R_M, C_M) and specifi c cytoplasm (axial) resistance (R_A). In the compartmental representation, the tree is discretized into a set of interconnected R-C compartments. Each is a lumped representation of the membrane properties of a suffi ciently small dendritic segment. Compartments are connected via axial cytoplasmic resistances. In this approach, the voltage can be computed at each compartment for any (nonlinear) input and for voltage and time-dependent membrane properties.

A discussion of the numerical techniques used by GENESIS to solve this set of equations is given in Chapter 20.

5.6   Compartmental Modeling Experiments

Having covered the basics of cable theory and compartmental modeling, we are now ready to try some computer "experiments" that will help us to better understand the previous sections. The GENESIS *Cable* tutorial implements a dendritic cable model that has been converted to an equivalent cylinder. Thus, it creates a one-dimensional compartmentalized cable similar to a single branch of the dendritic tree shown in Fig. 5.4C. Each cylindrical compartment is similar to the one shown in Fig. 2.3, with the axial resistance on the left side of the compartment and with the resting membrane potential E_m set to zero. You can provide a current injection pulse to any compartment, setting the delay, pulse width and amplitude from a menu. Although we won't make use of it in this chapter, you may also provide a synaptic input, corresponding to the variable resistor in series with a battery shown in Fig. 2.3.

   The cable consists of a "soma" compartment and N identical "cable" compartments. You can set N to be any number you like, and can separately modify the length and diameter for the soma and for the identical cable compartments. You can also set the specific axial and membrane resistances and specific membrane capacitance. These values apply to both the soma and cable compartments. The soma compartment is labeled as compartment 0, and is the leftmost compartment, located at $X = 0$. This means that the axial resistance of the soma compartment doesn't enter into the calculation — all compartments communicate through the axial resistances of the dendritic cable. This also means that the rightmost compartment, compartment N at $X = L$, can have no current flow to the right. Thus, our model corresponds to the sealed end boundary condition discussed in Sec. 5.4.1.

   As always, the best way to understand the model is to run the simulation. Before reading further, you should start the *Cable* simulation from a terminal window at the bottom of your screen. This is done by changing to the *Scripts/cable* directory and typing "`genesis Cable`." After a slight delay, a control panel and two graphs will appear. If you click the mouse on both the `Change Cell Parameters` and `Change Current Injection` buttons, two more windows should appear, resulting in a display similar to the one shown in Fig. 5.5.

   As with most of the tutorials, the `HELP` button will call up a menu with a number of selections, including `Running the Simulation`. You may use this to get a description of the uses of the various buttons, toggles and dialog boxes. Take a few minutes to understand what the default values of the cable parameters are, and the units that are being used. Note that the `Cable Compts.` dialog box shows "`0`," indicating that there is only a single soma compartment. The dialog boxes in the `Cell Parameters` menu at the upper right indicate
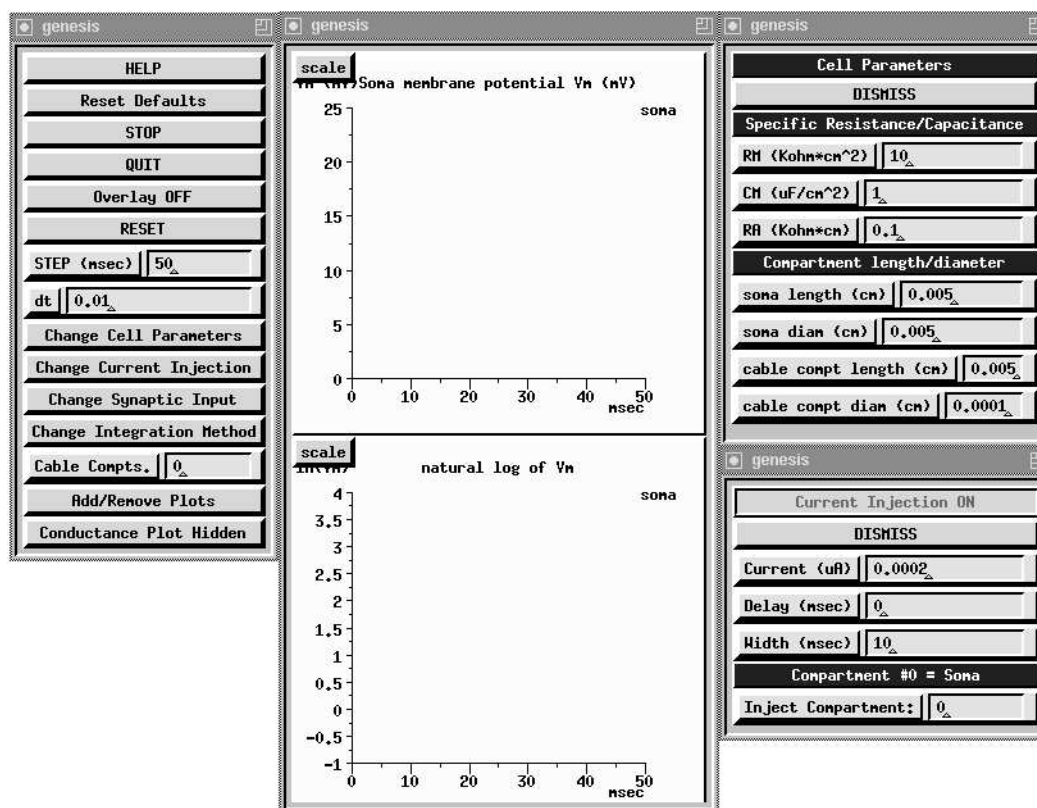
Figure 5.5 A display from the GENESIS *Cable* tutorial, showing the default values of various parameters. The `Change Cell Parameters` and `Change Current Injection` buttons on the control panel (to the left) were used to call up the two menus on the right.

that it has a length and diameter both equal to 50 *μm* (0.005 *cm*). Later, we will add dendritic cable compartments and change some of the parameters.

Try hitting "Return" while the cursor is in the data field of one of the dialog boxes in the `Cell Parameters` menu. This would normally be done after changing some of the dialog boxes for the compartment dimensions or the specific resistances and capacitances, so that the values of R_m, C_m and R_a will be recomputed. It also causes these values to be displayed in the terminal window. Can you satisfy yourself that they are the ones expected from Eqs. 5.4–5.6? The menu at the lower right indicates that, with no delay, a current of 0.2 *nA* will be injected to the soma for 10 *msec*. Can you predict what the plots of $V(t)$ and $\ln(V(t))$ will look like? What will be the maximum value of $V(t)$? What do you expect the slope of the logarithmic plot to be after the end of the injection pulse? After you have made these estimates, go ahead and click on `STEP` to perform the simulation for

50 *msec*. Now, measure the quantities that you have predicted. If the values are not within reasonable agreement with theory, take the time to correct your mistakes, or to understand what went wrong. (Hint: use the `scale` button to call up the graph scale menu, or click and drag the mouse along a graph axis to zoom in to a region in order to make more accurate measurements. It may be helpful to use a small ruler with a millimeter scale to help with interpolation. If your computer has the ability to capture and print portions of the screen image, this will make these measurements even easier.)

After this "warm-up" exercise, we are ready to perform a more interesting experiment. Now, add a dendritic cable to the soma by changing the `Cable Compts.` dialog box contents to "`10`." Keep the original dimensions for the soma compartment and also use the default values of the cable compartment dimensions (a diameter of 1 *μm* and length of 50 *μm*). You should be able to verify that each cable compartment has a length of 0.1λ, and that the electrotonic length of the entire cable is given by $L = 1$. Although we are not dealing with a steady voltage, nor with an infinite cable, Eq. 5.13 suggests that the change in voltage from one compartment to another will be relatively small with this size compartment, justifying our use of a compartmental model. Clearly, the question of how small we need to make the compartments is an important one. You may investigate this issue more carefully in Exercise 3, at the end of this chapter.

Before continuing, you should be aware of another factor that can affect the accuracy of your simulation. In previous chapters, we have referred to the importance of choosing an appropriate size for the integration time step (given in the `dt` dialog box). This is particularly true for cable models that contain many short compartments (Chapter 20, Sec. 20.3.4). Although the default time step should be adequate for the exercises suggested here, you should experiment with smaller values if you make significant changes in the cable parameters.

In order to compare the results to those obtained with only the isolated soma, click on `Overlay OFF` so that it changes to `Overlay ON`; then click on `RESET` and `STEP`. Do you expect the different dimensions of the cable to affect the decay of the voltage after the pulse? Can you explain any differences in the two plots of ln(V) right after the end of the injection pulse? You may explore this effect in more detail in Exercise 5.

Finally, let's examine the effect of the dendrite diameter on the propagation of voltage changes along the dendritic cable. For this, we would like a little sharper change in voltage, so increase the soma injection current to 2 *nA* (0.002 *μA*) and reduce the pulse width to 1 *msec*. In order to measure the potential at other places along the cable, click on the `Add/Remove Plots` button to bring up a menu that will allow you to specify other compartments in which to record the membrane potential. Note that the default is to record from the soma. By entering "`5`" and then "`10`" in the dialog box, you may add plots of V for these two compartments. Clicking on `Remove Cable Plots` removes plotting for all but the soma compartment. Having added these two extra plots, leave the cable diameter at 1 *μm* and run the simulation. Make a note of the maximum value of V_m and the time it

takes to reach this value for each of the three locations. Now, change the cable diameter to 0.5 *μm* and repeat the experiment. What is the electronic length *L* of the cable with this new diameter? How does the diameter affect the decay of the potential with distance? Can you explain this? By observing the change of position of the peak in *V* with distance, can you estimate the propagation velocity of the voltage deviation? How does the propagation velocity seem to depend on dendrite diameter?

There are a number of other experiments suggested at the end of the chapter that will shed more light on the effect the dendritic cable has upon the propagation of electrical signals. For example, Exercise 4 investigates the asymmetry of propagation from soma to dendrites as compared to propagation in the opposite direction, as seen in Fig. 5.3A. Exercise 6 studies the effect of the cable on the input resistance of the neuron. In Exercise 7, we make use of the broadening of potentials as they propagate away from the point at which they were introduced (Fig. 5.3B) to estimate dendritic lengths.

5.7   Main Insights for Passive Dendrites with Synapses

Here we summarize the main insights regarding the input-output properties of passive dendrites, gained from modeling and experimental studies on dendrites during the last forty years.

1. Dendritic trees are electrically distributed (rather than isopotential) elements. Consequently, voltage gradients exist over the tree when synaptic inputs are applied locally. Because of inherent non-symmetric boundary conditions in dendritic trees, voltage attenuates much more severely in the dendrites-to-soma direction than in the opposite direction (Fig. 5.3A). In other words, from the *soma* viewpoint, dendrites are electrically rather compact (average cable length *L* of 0.3–2 λ). From the *dendrite* (synaptic) viewpoint, however, the tree is electrically far from being compact. A corollary of this asymmetry is that, as seen in Fig. 5.3A, short side branches (in particular, dendritic spines) are essentially isopotential with the parent dendrite when current flows from the parent into these side branches (spines) but a large voltage attenuation exists from terminal (spine) to parent when the terminal receives direct input.

2. The large voltage attenuation from dendrites to soma (which may be a few hundred-fold for brief synaptic inputs at distal sites) implies that many (several tens) of excitatory inputs should be activated within the integration time window τ_m, in order to build up depolarization of 10–20 *mV* and reach threshold for firing of spikes at the soma and axon (e.g., Otmakhov, Shirke and Malinow 1993, Barbour 1993). The large local depolarization expected at the dendrites, together with the marked atten-

uation in the tree imply that the tree can be functionally separated into many, almost independent, subunits (Koch, Poggio and Torre 1982).

3. Although severely attenuated in peak values, the attenuation of the area of transient potentials (as well as the attenuation of charge) is relatively small. The attenuation of the area is identical to the attenuation of the steady voltage, independently of the transient shape (Rinzel and Rall 1974). Comparing the steady-state somatic voltage that results from distal dendritic input to the soma voltage when the same input is applied directly to the soma (dashed line in Fig. 5.3A) highlights this point. Thus, the "cost" (in term of area or charge) of placing the synapse at the dendrites rather than at the soma is quite small.

4. Linear system theory implies an interesting reciprocity in passive trees. The voltage at some location x_j resulting from transient current input at point x_i is identical to the voltage transient measured at x_i when the same current input is applied at x_j (Koch et al. 1982). Because the input resistance is typically larger at thin distal dendrites and in spines than at proximal dendrites (and the soma), the same current produces a larger voltage response at distal dendritic arbors. Thus, the reciprocity theorem implies that the *attenuation* of voltage from these sites to the soma is steeper than in the opposite direction (i.e., asymmetrical attenuation). Reciprocity also holds for the total signal delay between any given points in the dendritic tree (Agmon-Snir and Segev 1993).

5. Synaptic potentials are delayed, and they become significantly broader, as they spread away from the input site (Fig. 5.3B). The large sink provided by the tree at distal arbors implies that, locally, synaptic potentials are very brief. At the soma level, however, the time-course of the synaptic potentials is primarily governed by τ_m. This change in width of the synaptic potential implies multiple time windows for synaptic integration in the tree (Agmon-Snir and Segev 1993).

6. Excluding very distal inputs, the cost (in terms of delay) that results from dendritic propagation time (i.e., the net dendritic delay) is small compared to the relevant time window (τ_m) for somatic integration. Thus, for the majority of synapses, the significant time window for *somatic* integration remains τ_m (Agmon-Snir and Segev 1993).

7. Because of the inherent conductance change (shunt) associated with synaptic inputs, synaptic potentials sum nonlinearly (less than linear) with each other (Chapter 6). This local conductance change of the membrane is better "felt" by electrically adjacent synapses than by more remote (electrically decoupled) synapses. Consequently, in passive trees, spatially distributed excitatory inputs sum more linearly (produce more charge) than do spatially clustered synapses (Rall 1964).

8. Inhibitory synapses (whose conductance change is associated with a battery near the resting potential) are more effective when located on the path between the excitatory input and the "target" point (soma) than when placed distal to the excitatory input. Thus, when strategically placed, inhibitory inputs can specifically veto parts of the dendritic tree and not others (Rall 1964, Koch et al. 1982, Jack et al. 1975).

9. Because of dendritic delay, the somatic depolarization that results from activation of excitatory inputs at the dendrites is very sensitive to the temporal sequence of the synaptic activation. It is largest when the synaptic activation starts at distal dendritic sites and progresses proximally. Activation of the same synapses in the reverse order in time will produce smaller somatic depolarization. Thus, the output of neurons with dendrites is inherently directionally selective (Rall 1964).

10. Because the synaptic input changes the membrane conductance, it effectively alters the cable properties (electrotonic length, input resistance, time constant, etc.) of the postsynaptic cell. This activity can reduce the time constant by a factor of 10 (Bernander et al. 1991, Rapp et al. 1992). Thus, spontaneous (background) synaptic activity dynamically changes the computational (input-output) capabilities of the neuron.

5.8 Biophysics of Excitable Dendrites

A growing body of experimental evidence in recent years has clearly demonstrated that the membrane of many types of dendrites is endowed with voltage-gated (nonlinear) ion channels, including the NMDA channels as well as voltage-activated inward (Ca^{+2} and Na^+) and outward (K^+) conductances (e.g., Stuart and Sakmann 1994, Laurent 1993, McKenna et al. 1992, Wilson 1992). These channels are responsible for a variety of subthreshold electrical nonlinearities and, under favorable conditions, they can generate full-blown action potentials. The use of voltage- and ion-dependent dyes as well as intracellular and patch-clamp recordings from dendrites suggested that, in contrast to axonal trees, the regenerative phenomenon from input into excitable dendrites tends to spread only locally. This makes functional sense since, otherwise, the dendritic tree would be essentially no different from the axon, implementing a simple all-or-none operation. However, because of the asymmetric spread of voltages within the dendritic tree (Fig. 5.3A) and because of inhomogeneous distribution of excitable channels in dendrites, spikes can propagate more readily back from the soma to the dendrites (Stuart and Sakmann 1994). Unfortunately, we still lack information regarding the distribution, the voltage-dependence, and the kinetics of excitable channels in dendrites and most of the results of this section are primarily based on theoretical predictions.

What is the electrical behavior to be expected from dendrites with voltage-gated membrane ion channels? First, we note that the presence of voltage-gated channels in dendrites

does not automatically imply that these channels participate in the electrical activity of the tree under all conditions. The large conductance load imposed by the tree effectively increases the activation threshold of these channels for local synaptic potentials (Rall and Segev 1987). These channels will be more readily activated under favorable conditions such as in regions with high densities of excitable channels (as in the initial segment of the axon), when the excitable channels have fast activation kinetics, or when the input is distributed (not localized). When activated, these channels can modulate the input-output properties of the neuron. For example, they can *amplify* the excitatory synaptic current and, for channels that carry inward current, the regenerative activity can spread ("chain reaction") and indirectly activate nearby dendritic regions that will further enhance the excitatory synaptic inputs (Rall and Segev 1987). Consequently, distal excitatory synaptic inputs may be less attenuated and, thus, affect more strongly the neuron output than would be expected in the passive case. In general, because of the asymmetry of voltage attenuation in dendritic trees (Fig. 5.3A), regenerative activity in dendrites will spread more securely in the centrifugal (soma-to-dendrites) direction than in the centripetal direction. This effect may be explored in the simulation (*traub91*) of the CA3 pyramidal cell described in Chapter 7. In addition to modulating the strength of the synaptic current, the kinetics of excitable channels may also play an important role in modulating the *speed* of electrical interaction in the dendritic tree.

Another consequence of dendritic nonlinearity was discussed by Mel (1993). Unlike the passive case where synaptic saturation implies loss in synaptic efficacy when the synapses are spatially clustered (see number 7 above), in the excitable situation (including the case of the voltage- and transmitter-gated NMDA receptors) a certain degree of input clustering implies more charge transfer to the soma (due to the extra active inward current). In this case, the output at the axon depends sensitively on the size (and site) of the "clusteron" and this may serve as a mechanism for implementing a multi-dimensional discrimination task of input patterns via multiplication-like operation.

Recently, the possibility that active dendritic currents (both inward and outward) may serve as a mechanism for synaptic gain control was put forward by Wilson (1992) in the context of neostriatal neurons and by Laurent (1993) for the axonless nonspiking interneurons of the locust. The principal idea is that, as a result of active currents, the integrative capabilities of the neuron (e.g., its input resistance and electrotonic length) are dynamically controlled by the membrane potential; thereby the neuron output depends on its state (membrane potential). Active currents (e.g., outward K^+ current) can act to counterbalance excitatory synaptic inputs (negative feedback) and thus stabilize the input-output characteristics of the neuron. Conversely, at other voltage regimes, active currents might effectively increase the input resistance and reduce the electrotonic distance between synapses (positive feedback) with the consequence of nonlinearly boosting a specific group of coactive excitatory synapses.

5.9 Computational Function of Dendrites

It seems appropriate to conclude this chapter by asking what kind of computations could be performed by a neuron with dendrites that could not be carried out with just a formless point neuron. Several answers have already been discussed; here the major ones are succinctly highlighted:

1. Neurons with dendrites can compute the direction of motion (Rall 1964, Koch et al. 1982).

2. Neurons with dendrites can simultaneously function on multiple time windows. For local dendritic computations (e.g., triggering local dendritic spikes, triggering local plastic processes) distal arbors act more as coincidence detectors, whereas the soma acts more as an integrator when brief synaptic inputs (i.e., non-NMDA and $GABA_A$) are involved (Agmon-Snir and Segev 1993).

3. Neurons with dendrites can implement a multi-dimensional classification task (Mel 1993).

4. Neurons with dendrites can function as many, almost independent, functional sub-units. Each unit can implement a rich repertoire of logical operations (Koch et al. 1982, Rall and Segev 1987) as well as other local computations (e.g., local synaptic plasticity) and they can function as semi-autonomous input-output elements (e.g., via dendrodendritic synapses).

5. Neurons with slow ion currents in the dendrites that are partially decoupled from fast spike-generating currents at the soma/axon hillock can produce a large repertoire of frequency patterns. By modulating the degree of electrical coupling between the dendrites and the soma (e.g., by inhibition) the same input can produce regular high frequency spiking as well as bursting — as thought to occur in experimental and theoretical models of epileptic seizures (Pinsky and Rinzel 1994).

5.10 Exercises

1. Plot the theoretical attenuation of steady voltage as a function of physical distance in infinitely long cylindrical cables with $R_M = 10,000\ \Omega \cdot cm^2$ and $R_A = 100\ \Omega \cdot cm$. Make plots for the three cable diameters, $d = 0.5\ \mu m$, $1\ \mu m$ and $2\ \mu m$. What can you conclude about the effect of dendritic diameter on the passive propagation of voltages? How does this compare with the results of the experiment on the finite cable discussed in Sec. 5.6?

2. (a) Calculate the input resistance of infinite cylindrical cables with $d = 0.5$ *μm*, 1 *μm*
   and 2 *μm*. As in the preceding exercise, assume $R_M = 10,000$ $\Omega \cdot cm^2$ and $R_A = 100$ $\Omega \cdot cm$.

   (b) Calculate the input resistance of two identical daughter branches of the above
   cylinder that obey Eq. 5.25.

   (c) Calculate the input resistance at $X = 0$ of a finite cylinder with $d = 1\mu m$, $R_M = 10,000$ $\Omega \cdot cm^2$ and $R_A = 100$ $\Omega \cdot cm$. Examine both the case of a sealed end at $X = 1$
   and the case of an end that is clamped to rest ($V = 0$) at $X = 1$.

   (d) Which of the input resistances calculated in (a) and (c) is closest to the result for
   the finite cable that we simulated in Sec. 5.6? Explain any similarities and differences.

3. One of the first questions to be answered before using or constructing a compartmen-
   tal model is, "What value of l is small enough to allow the approximation of Eq. 5.27
   with Eq. 5.28?" This question can be answered by performing "computer experi-
   ments" on a system for which we know the exact solution. Equation 5.14 gives the
   exact result for the attenuation of a steady-state membrane potential with distance for
   a uniform finite length cable. In order to make the simulated cable a uniform one,
   change the soma dimensions to make it the same size as a dendritic compartment.
   Then add 10 cable compartments to the soma, using the default values of all the pa-
   rameters. Explain why, although there are now 11 compartments, including the soma,
   the electrotonic length of this cable is $L = 1$, and not $L = 1.1$.

   Set the value of the current injection to the soma at 0.0001 *μA* (0.1 *nA*), and set the
   width of the injection pulse to a large value, so that there will be a constant injection
   current. Plot the membrane potential in both the soma and the end compartment,
   and calculate the steady-state ratio of $V(L)/V(0)$. How does it compare with the
   prediction of Eq. 5.14?

   Now, repeat the experiment with 5 and then 20 cable compartments, changing the
   compartment length to keep the total electrotonic length of the cable at $L = 1$. What
   do you conclude is a good practical definition of "small enough"?

4. Restore the default parameters for the *Cable* simulation (soma length and diameter of
   50 *μm*; cable compartment diameter of 1 *μm* and length of 50 *μm*). Make a cable with
   10 dendritic compartments, and provide a 2 *msec* pulse of 0.1 *nA* current injection
   to the soma, recording the membrane potential at both the soma and compartment
   10. Then change the injection point to compartment 10, toggle to `overlay ON`, click
   on `RESET` and run the simulation again. Make an estimate of the attenuation of the
   voltage in the soma-to-dendrite direction and then in the opposite direction. Finally,
   repeat the experiment with the dendritic cable diameter set to 0.5 *μm*. What accounts

for the different attenuation in the two directions? Why is the dendritic diameter relevant? What significance do these results have for neuronal behavior?

5. Use the uniform cable ($L = 1$) from Exercise 3 and apply a brief (2 *msec*) current injection to the soma. Use the `Add/Remove Plots` menu to plot $V(t)$ from compartments 0, 5 and 10. Examine the plot of $\ln(V)$ vs. t and note that the response is not a simple exponential. Explain why the three logarithmic plots have different curvatures at the start of the voltage decay, and account for the direction of each.

   Now, record only from the soma, and generate overlaid logarithmic plots for cables of length $L = 0.5$, 1 and 2 (5, 10 and 20 compartments). Explain why some of these show a linear slope at earlier times than others.

6. Use the *Cable* simulation to construct a uniform cable like the one in Exercise 3 and perform an experiment to measure the input resistance at the soma ($X = 0$). Use this value to calculate the specific membrane resistance R_M for the cable and compare it to the value that was actually used in the simulation.

7. Using the *Cable* simulation, add 15 cable compartments, each 0.1λ long, to the soma compartment. Place your recording electrode at compartment 0 ("soma") and inject a brief current pulse once at compartment 0, then at 5, 10 and 15. Measure the peak time (PT) and half width (HW) of the somatic voltage for the different cases and plot PT vs. HW for the different X values. Label each data point with the X value to which it corresponds. Do some interpolation. Can you predict the result for compartment 8 with any accuracy?